

# Effects of the Bogie and Body Inertia on the Nonlinear Wheel-set Hunting Recognized by the Hopf Bifurcation Theory

D. Younesian<sup>1,\*</sup>, A. A. Jafari<sup>2</sup> and R. Serajian<sup>3</sup>

<sup>1</sup> Associate Professor, School of Railway Engineering, Iran University of Science and Technology

<sup>2</sup> Associate Professor, <sup>3</sup>MSc Student, Department of Mechanical Engineering, K. N. T. University of Technology

\* younesian@iust.ac.ir

## Abstract

Nonlinear hunting speeds of railway vehicles running on a tangent track are analytically obtained using Hopf bifurcation theory in this paper. The railway vehicle model consists of nonlinear primary yaw dampers, nonlinear flange contact stiffness as well as the clearance between the wheel flange and rail tread. Linear and nonlinear critical speeds are obtained using Bogoliubov method. A comprehensive parametric study is then carried out and the effects of different parameters like the magnitudes of lateral clearance, damping values, wheel radius, bogie mass, lateral stiffness and the track gauge on linear and nonlinear hunting speeds are investigated.

*Keywords: Bifurcation, Critical speed, Nonlinear, Hunting, Bogoliubov method.*

## 1. INTRODUCTION

Dynamic stability analysis of high-speed trains has recently received remarkable attentions due to its importance and critical role in railway transit. A preventive factor in high-speed railway vehicles has been proved to be “hunting” associated with a lightly damped lateral/yaw response of the bogie wheel-set. The wheel-set hunting can consequently cause the wheel climb and eventually it can lead to the train derailment. High speed demands in conjunction with the higher axle loads have enhanced nowadays the possibility of this type of dynamic instability both in passenger and freight trains. Surveying the literature reveals that a remarkable number of studies have been conducted so far in dynamic stability analysis of railway vehicles. A comprehensive history of stability of railway vehicles presenting a retrospective view in last two centuries has been provided by Knothe and Bohm in [1]. A numerical bifurcation analysis has been carried out and the chaotic dynamic behavior of the wheelset has been evaluated as a function of the vehicle speed, suspension stiffness, and flange forces by Knudsen et al [2]. Effects of nonlinear yaw dampers and wheel-rail interface on critical speeds of a locomotive bogie have been numerically investigated by Ahmadian and Yang in [3]. An analytical investigation of Hopf bifurcation and hunting behavior of a single wheel-set with nonlinear

primary yaw dampers and wheel/rail contact forces has been presented by Ahmadian and Yang in [4]. Stabilization control for the hunting motion of a railway wheel-set has been studied by Yabuno et al. in [5, 6]. A passive non-linear elastic suspension device has been proposed by Scheffel [7] in order to improve hunting stability of railway bogies. Hunting stability of a Y-25 freight wagon has been numerically analyzed by Molatefi et al. [8] in the time domain. Lee and Cheng [9-14] employed eigenvalue characterization method and numerically studied nonlinear hunting in different types of high-speed railway vehicles travelling on varieties of tangent and curved tracks. Effects of hollow wheels on wheel/rail contact geometry and on the vehicle stability have been investigated by Sawley et al. [15]. Kim and Seok [16] employed method of multiple scales and numerically analyzed the bifurcation and hunting behavior of a dual-bogie railway vehicle. Flexibility of the railway track was included in a research conducted by Zhai et al. [17, 18] and Shabana et al. [19, 20] critical hunting speed of a freight car with three-piece bogies running on an elastic track was obtained. More recently, Younesian et al. [21, 22] numerically analyzed dynamic stability and derailment of partially filled tanker trains running on tangent and curved tracks. The primary purpose of the present study is to extend the results in the literature by including the nonlinear dynamics of flange contact in presence of

bogie and body inertia. Nonlinear hunting analysis of a single wheel-set (earlier studied in the literature) has been corresponding to an infinite inertia for the bogie and body and consequently both of them have been assumed to be stationary. The secondary objective of this research is to provide a comprehensive parametric study for further investigation into the effects of different parameters on the nonlinear hunting speed.

Although the nonlinear contact models have been already employed in literature but the bogies are assumed to be fixed in spatial space. Accordingly using this assumption, the effects of bogie and body mass are neglected in modeling and simulation. Validity and range of application for this assumption is investigated in this paper.

The nonlinearity arises from dynamic behavior of the yaw dampers and also the interactive forces in contact zone. Nonlinear governing equations of motion are derived and discussed in the first section followed by a brief review on stability analysis based on the Hopf bifurcation theory. In order to provide a parametric study, series of numerical simulations are carried out after verification of the solution procedure. Effects of different parameters such as un-sprung inertia, bogie inertia, body inertia, wheel radius, stiffness and damping of the secondary and primary suspension systems on both the linear and nonlinear hunting speeds are evaluated.

## 2. GOVERNING EQUATIONS OF MOTION

A wheelset with lateral and yaw degrees of freedom is combined with a bogie and body as illustrated in Figure 1. Using the nonlinear contact model [3, 23] for the wheel/rail interaction the nonlinear governing equations of motion can be derived as:

$$\begin{cases} \ddot{y} + 2K_y y + 2C_y \dot{y} = 0 \\ \ddot{\psi} + 2K_\psi \psi + 2C_\psi \dot{\psi} = 0 \end{cases} \quad (1)$$

in which:

$$F = -2K_y y - 2C_y \dot{y}, \quad (2)$$

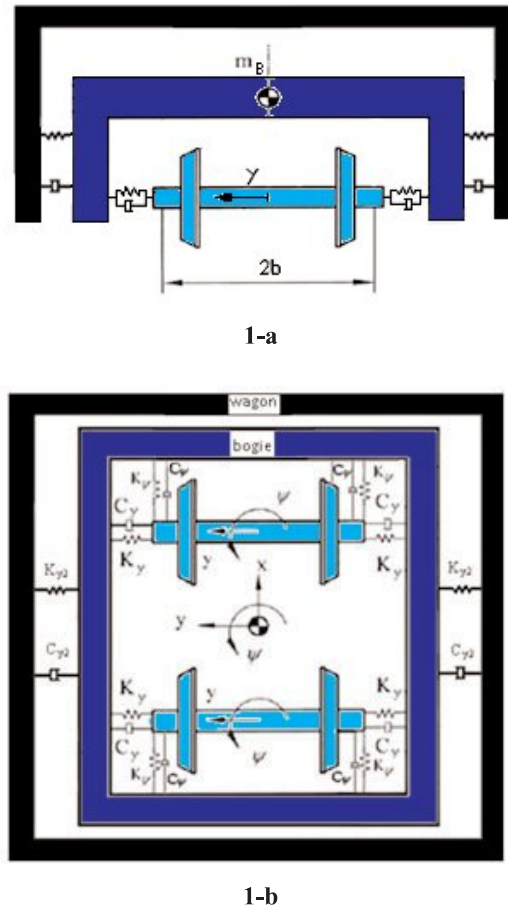


Fig. 1. Body, bogie and wheelset configuration, (a) Front view, (b) Upward view.

The flange contact force  $F_T$  is modeled as a nonlinear spring with dead-band equal to the flange clearance i.e.

$$F = \begin{cases} K(y - \delta); & y > \delta \\ 0; & -\delta \leq y \leq \delta \\ K(y + \delta); & y < -\delta \end{cases} \quad (3)$$

where  $K_r$  and  $\delta$  are respectively the rail lateral stiffness and flange clearance. Yaw differential equation of motion can be then expressed as:

$$M \ddot{\psi} = -2K_\psi \psi - 2C_\psi \dot{\psi}, \quad (4)$$

The nonlinear longitudinal yaw damping force  $F_d$  can be defined by [3]:

$$F_d = \begin{cases} C_V V + C_V V + C_V V + C_V V; & V > 0 \\ C_V V - C_V V - C_V V - C_V V; & V < 0 \end{cases} \quad (5)$$

Where  $V = b\psi$ . The nonlinear equations of motion are expressed in the state space so that the state vector is selected to be:

$$X = \begin{bmatrix} x \\ \dot{x} \\ x \\ \dot{x} \\ x \\ \dot{x} \\ x \\ \dot{x} \\ x \\ \dot{x} \end{bmatrix} = \begin{bmatrix} y \\ \dot{y} \\ \psi \\ \dot{\psi} \\ z \\ \dot{z} \\ x \\ \dot{x} \end{bmatrix} \quad (6)$$

Accordingly, the nonlinear equations are converted into:

$$\dot{X} = A(V)X + F(X) \quad X \in R, \quad (7)$$

In which the matrix equations are divided into two parts of linear and nonlinear ones.  $F(X)$  denotes the nonlinear terms and the elements of the matrix  $A(V)$  are described as:

$$\begin{bmatrix} \ddots & \ddots & \ddots & \ddots & \ddots & \ddots \\ \ddots & \ddots & \ddots & \ddots & \ddots & \ddots \\ \ddots & \ddots & \ddots & \ddots & \ddots & \ddots \\ \ddots & \ddots & \ddots & \ddots & \ddots & \ddots \\ \ddots & \ddots & \ddots & \ddots & \ddots & \ddots \\ \ddots & \ddots & \ddots & \ddots & \ddots & \ddots \end{bmatrix} \quad (8)$$

Defining  $V$  and  $V_C$  to be respectively the nonlinear and linear hunting speeds and perturbing  $V$  around  $V_C$  one can arrive to:

$$V = V_C + \varepsilon\mu \quad (9)$$

in which  $\mu$  the detuning parameter. Accordingly, the state matrix can be expanded by

$$A(V) = A(V_C) - \varepsilon\mu A'(V_C) + (\varepsilon\mu)^2 A''(V_C) \mp \dots \quad (10)$$

Combining equations (7) and (9) gives:

$$\dot{X} = A(V_C)X + \varepsilon F(X; \mu, \varepsilon); X \in R, \quad (11)$$

Where

$$\begin{bmatrix} \ddots & \ddots & \ddots & \ddots & \ddots & \ddots \\ \ddots & \ddots & \ddots & \ddots & \ddots & \ddots \\ \ddots & \ddots & \ddots & \ddots & \ddots & \ddots \\ \ddots & \ddots & \ddots & \ddots & \ddots & \ddots \\ \ddots & \ddots & \ddots & \ddots & \ddots & \ddots \\ \ddots & \ddots & \ddots & \ddots & \ddots & \ddots \end{bmatrix}$$

By using the Bogoliubov method [24], the solutions can be approximated by:

$$\begin{bmatrix} y(t) \\ \dot{y}(t) \\ \psi(t) \\ \dot{\psi}(t) \\ z(t) \\ \dot{z}(t) \\ x(t) \\ \dot{x}(t) \end{bmatrix} = 2a(t) \begin{bmatrix} \alpha \\ \alpha \\ \alpha \\ \alpha \\ \alpha \\ \alpha \\ \alpha \\ \alpha \end{bmatrix} \cos(\varphi(t)) - \begin{bmatrix} \beta \\ \beta \\ \beta \\ \beta \\ \beta \\ \beta \\ \beta \\ \beta \end{bmatrix} \sin(\varphi(t)); \varphi = \omega t + \theta \quad (12)$$

Where  $\theta$  is determined by initial condition,  $\alpha_i$ s are real parts and  $\beta_i$ s are imaginary parts of

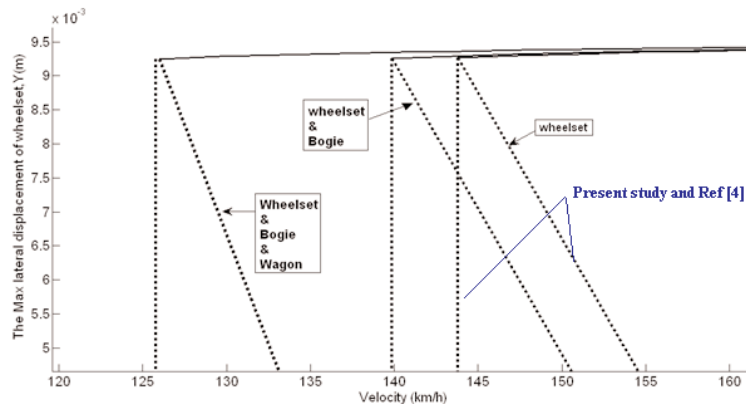


Fig. 2. Difference between hopf bifurcation diagrams for three different systems.

eigenvectors for  $A_o(V_c)$ .  $a(t)$  and  $\varphi(t)$  are obtained by first-order approximation:

$$\frac{da}{dt} = \varepsilon A_1(a), \quad \frac{d\varphi}{dt} = \omega + \varepsilon B_1(a), \quad (13)$$

in which,  $A_1(a)$  and  $B_1(a)$  are obtained by:

$$A(a) = \frac{1}{2\pi} \int \sum f(p \cos\varphi + q \sin\varphi) d\varphi, \quad (14)$$

$$B(a) = \frac{1}{2\pi a} \int \sum f(q \cos\varphi - p \sin\varphi) d\varphi,$$

$p_i$ s represent real parts and  $q_i$ s are imaginary parts of  $A_o^T(V_c)$ 's eigenvectors. Matrix equation of  $A_1(a)=0$  is numerically solved and the corresponding limit cycles are obtained. Stability of the limit cycles can be consequently checked by the following condition.

———  $< 0$ ,  $\rightarrow$  Stable Solution      ———  $> 0$ ,  $\rightarrow$  Unstable Solution

### 3. NUMERICAL RESULTS

Series of numerical simulations are directed in this section to provide a comprehensive parametric study on the linear and nonlinear hunting speeds. At the first part, effects of neglecting the bogie and body degrees

of freedom are focused. Figure (2) shows the bifurcation diagram for three different systems i.e. 1- single wheelset, 2- bogie-wheelset and 3-body-bogie-wheelset. Employing the Bogoliubov approach, the linear and nonlinear hunting speeds are obtained for three systems and listed in Table 1.

The obtained values not only verify validity of the solution procedure for a single wheelset [4] but also they prove that both the bogie and body degrees of freedom may remarkably reduce hunting speeds. "Figure 2 is emphasizing that neglecting the body and bogie motions in modeling could lead to significant difference between the reality and simulation. This assumption is predicting the critical speed wrongly being 144 km/hr instead of 126 km/hr." This reductive effect is enhanced in case of the nonlinear hunting. In other words, modelling of a single wheelset reduces the safety thresholds in vehicle designs against derailment. Effects of different parameters on both linear and nonlinear hunting speeds are evaluated in the following sections.

#### 3. 1. Un-sprung Mass

Effects of un-sprung mass in conjunction with the lateral stiffness on the hunting speeds are illustrated in Figure 3. It is seen that, by increasing lateral stiffness in primary suspension system, both linear and

Table 1. Mechanical properties of the railway vehicle

Parameters	Value
wheelset conicity	$\lambda = 0.05$ rad
flange clearance	$\delta = 0.00923$ m
half of the primary yaw spring arm	$b = 1.00$ m
lateral damping of primary suspension	$C = 2.1 \times 10$
lateral rail stiffness	$K = 1.617 \times 10$
lateral stiffness of primary suspension	$K = 8.67 \times 10$
yaw spring stiffness of primary suspension	$K = 8.67 \times 10$
damping coefficients for primary yaw dampers	$C = 1.923 \times 10$ , $C = 5.14 \times 10$ , $C = -3.1127 \times 10$ , $C = 5.14 \times 10$
half of the track gauge	$d = 0.7176$ m
lateral creep force coefficient	$f = 6.728 \times 10$ N
spin creep force coefficient	$f = 1000$ N
lateral spin creep force coefficient	$f = 1.2 \times 10$ N.m
longitudinal creep force coefficient	$f = 6.728 \times 10$ N
roll moment of inertia of wheelset	$I = 625.7$ kg.m
spin moment of inertia of wheelset	$I = 133.92$ kg.m
wheelset mass	$m = 1800$ kg
bogie mass	$m = 4000$ kg
wagon mass	$m = 35000$ kg
wheel radius	$r = 0.533$ m
axle load	$W = 18000$ N
lateral stiffness of secondary suspension	$K_y = 350000$ N/m
lateral damping of secondary suspension	$C_y = 17500$ N.S/m

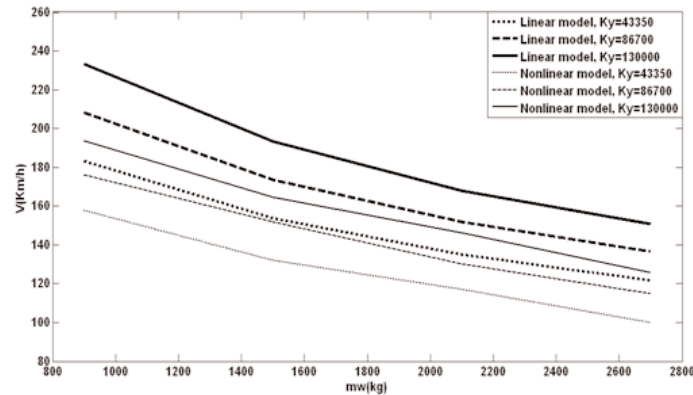


Fig. 3. Effect of un-sprung mass on critical speeds.

nonlinear critical speeds increase. In this case, increasing the un-sprung mass remarkably reduces both the linear and nonlinear hunting speeds. This behavior verifies lower potential of the lighter wheelsets to follow the hunting oscillatory motion.

### 3. 2. Wheelset Radius

Effects of wheel diameter on the hunting speeds are illustrated in Figure 4. It is seen that, increasing the wheel radius results in the larger hunting speeds. This means that for an identical wheelset offset with respect to the track centerline, the center of a larger wheel meets a smaller speed change percentage than the center of a smaller wheel. This means that any wheel grinding enhance possibility of the hunting in operation.

### 3. 3. Track Gauge

Numerical simulations demonstrate that the linear and nonlinear critical speeds respectively decrease and increase for wider track gauges (Figure 5). In other words, nonlinear hunting speeds converges to the linear ones in wider tracks. Effects of the intrinsic source of nonlinearity i.e. the clearance becomes weaker when its relative dimensions get smaller with respect to the track width dimension.

### 3. 4. Conicity

It is found that any larger equivalent conicity leads to lower critical speed up to a specific conicity value (Figure 6). Any larger conicity leads to larger speed difference between the two wheels and consequently it

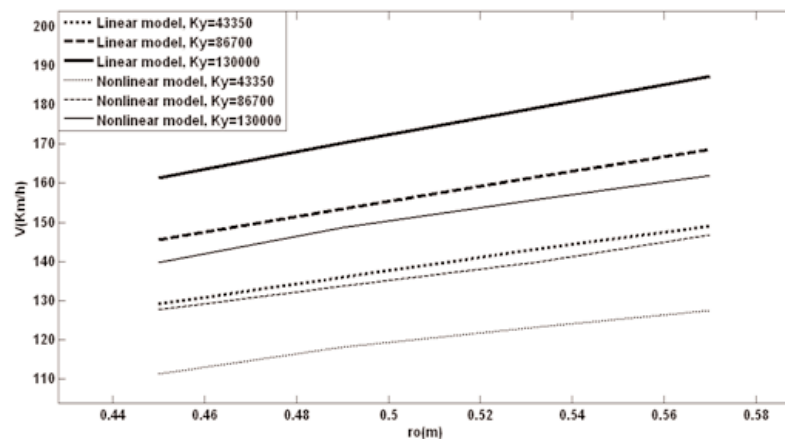


Fig. 4. Effect of wheel radius on critical speeds.

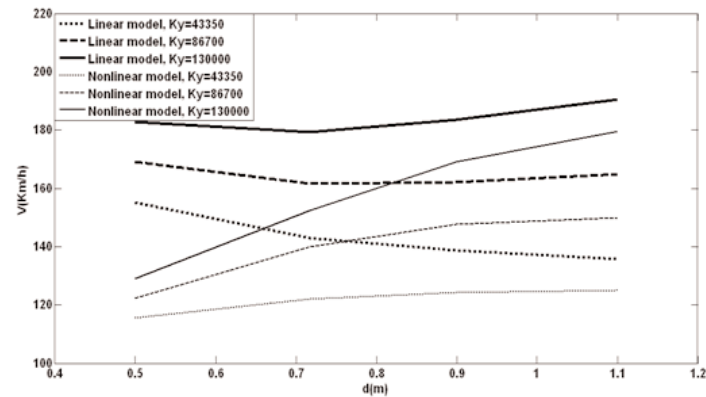


Fig. 5. Influence of the track gauge on the hunting behavior

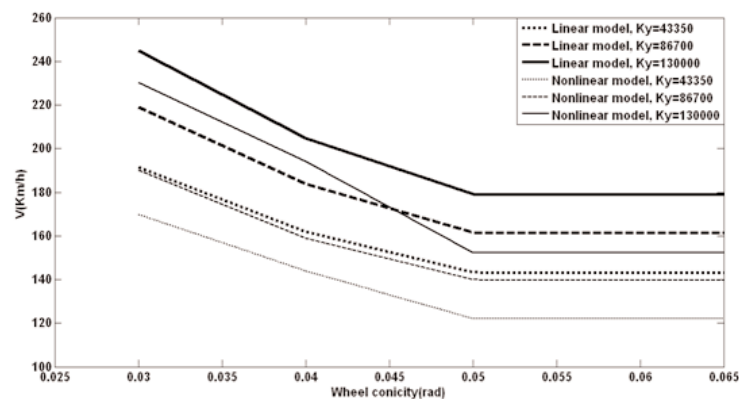


Fig. 6. Effects of the equivalent conicity on critical speeds

results in a higher potential to oscillatory hunting motion. Although increasing too much of conicity will not be effective, but it has a remarkable reductive effect both on the linear and nonlinear hunting speeds in low conicity range ( $<0.05$ ).

### 3. 5. Yaw Spring Stiffness of Primary Suspension

Effects of the yaw stiffness on the linear and nonlinear hunting speeds are illustrated in Figure 7. It is seen that both the linear and nonlinear hunting speeds are monotonically increasing functions of the yaw

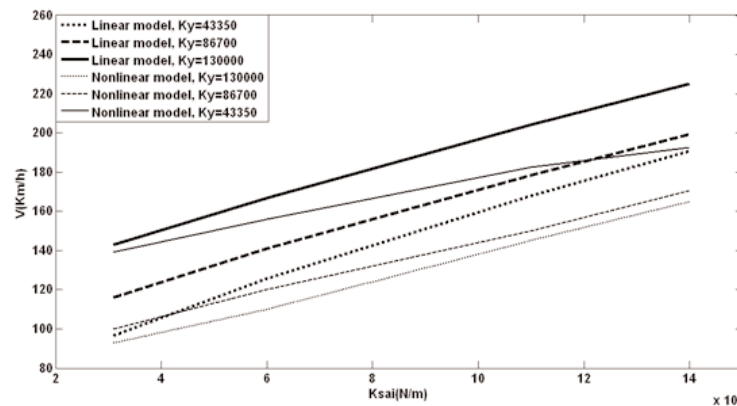


Fig. 7. Effects of yaw stiffness on hunting speeds

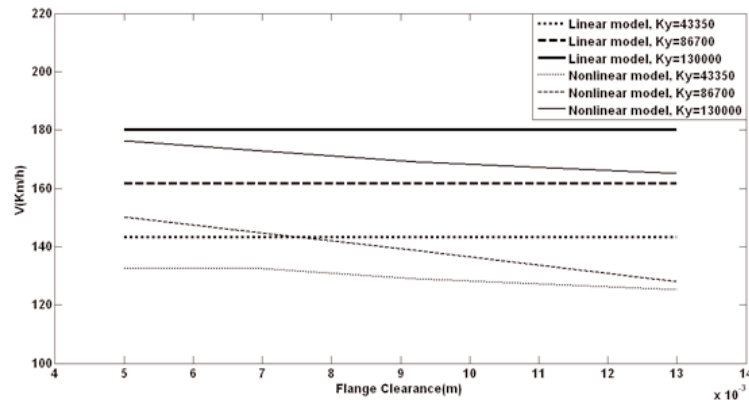


Fig. 8. Influences of the flange clearance on critical speeds

stiffness. This means that for an identical wheelset offset with respect to the track centerline, yaw stiffeners can remarkably constraint the hunting oscillatory motion of the wheelset. As a result, increasing the yaw stiffness can be employed as a control strategy in postponing the hunting phenomenon.

### 3. 6. Flange Clearance

Numerical simulations demonstrate that the flange clearance remarkably reduces the nonlinear speeds while it has no significant effect on the linear hunting speed (Figure. 10). The flange clearance can remarkably reduce the overall stiffness of the wheelset system in lateral direction and consequently it can enhance the possibility the hunting oscillatory motion in yaw direction. In other words, the linearized model has no sensitivity with respect to the flange clearance while the nonlinear model is correlated with what happens in reality.

It is also found that the rail stiffness has no significant effect neither on the linear nor on the nonlinear hunting speed.

### 3. 7. Secondary Lateral Stiffness and Damping

According to the Figures 9 and 10, increasing the lateral stiffness and damping in secondary suspension system leads to the larger values for both linear and nonlinear critical speeds. They have both a smaller influence on the hunting speed with respect to the primary suspension since they are not directly connected to the wheelset. An asymptotic behavior is observed for both sequence of variations with respect to the lateral stiffness and damping.

### 3. 8. Bogie Inertia

The objective in this section is to investigate how

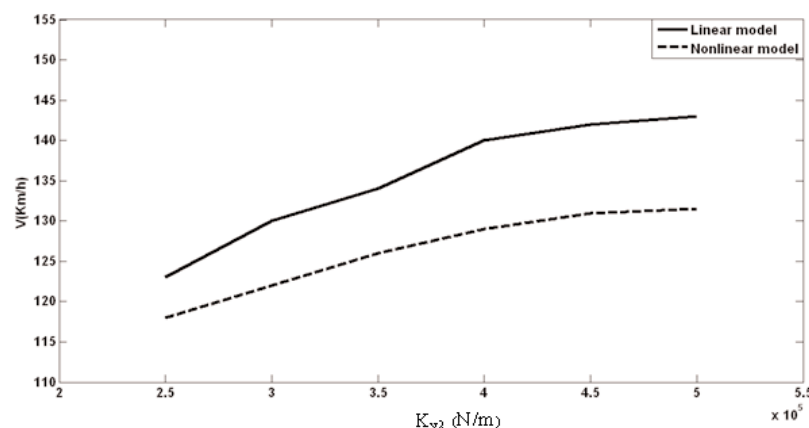


Fig. 9. Influence of lateral secondary suspension stiffness on hunting speeds



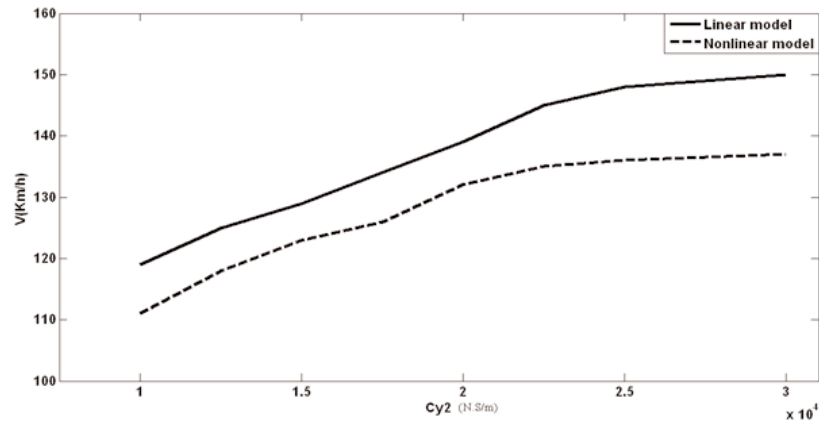


Fig. 10. Influence of lateral secondary suspension damping on the hunting speeds

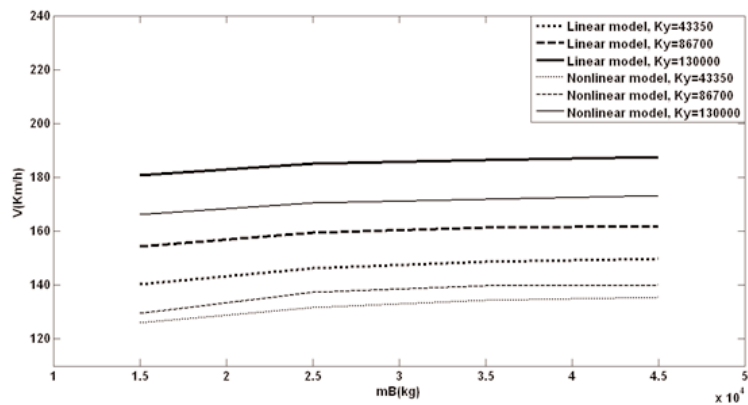


Fig. 11. Effects of the bogie mass on hunting speeds

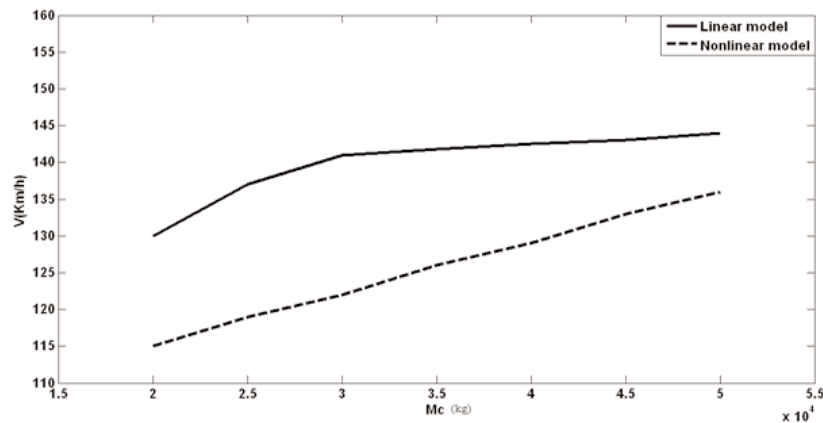


Fig. 12. Effects of body mass on hunting speeds

the bogie inertia can affect both the linear and nonlinear critical speeds. As shown in Figure 12, it is seen that both the critical speeds are asymptotically increasing functions of the bogie mass. This means

that heavier bogies can further restrict the lateral/yaw motion of the wheelset due to their larger inertia and resistance to motion.



### 3. 9. Body Inertia

As it was earlier discussed in Introduction, the bogie and also body are sometimes assumed to be a fixed support for the wheelset in the literature. The objective here in this section is to evaluate the order of error for such an assumption. Effects of the body mass on the linear and nonlinear hunting speeds are illustrated in Figure 11. As it is seen, the prescribed assumption may lead to a significant error in hunting estimations. For an infinite body-mass, the results coincide with those available in the literature based on the rigidity assumption. This means that the real hunting speeds is remarkably smaller than those obtained based on the rigidity assumption. In order to summarize the conducted sensitivity analysis, a parametric sweep is carried out in the range of  $\pm 50\%$  and the results are illustrated in Figures 13 and 14

respectively for linear and nonlinear model.

### 4. CONCLUSIONS

Hopf bifurcation theory was employed and nonlinear hunting speeds of a railway vehicle running on a tangent track were analytically obtained in this paper. A comprehensive parametric study was carried out and effects of different parameters on the linear and nonlinear hunting speeds were investigated. Two main matters i.e. assuming the body as a fixed support and influence of the nonlinear elements in calculation of the hunting speed were focused. It was found that the support assumption may lead to a significant error in hunting estimations. In other words, rigidity assumption leads to larger hunting speeds than reality and this underestimation can end up to a risky misinformation. Lateral stiffness and damping both in

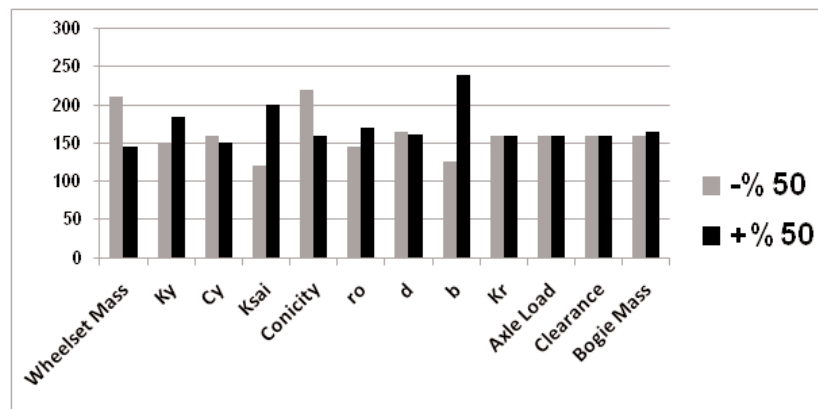


Fig. 13. Parametric study in linear model

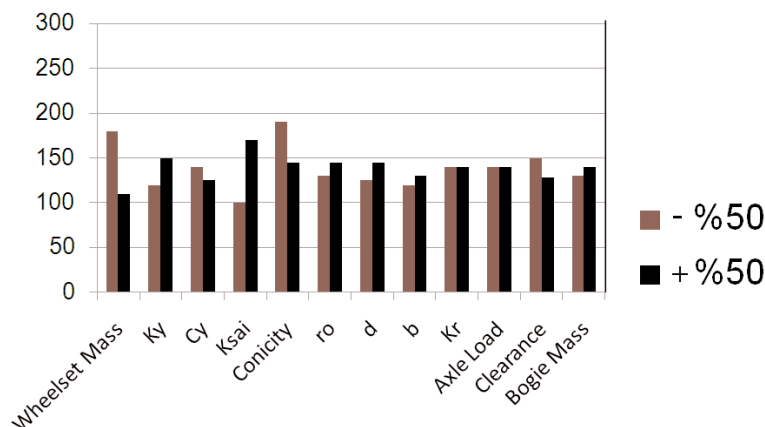


Fig. 14. Parametric study in nonlinear model.

primary and secondary suspension systems asymptotically enhance the nonlinear critical speeds. Increasing the un-sprung mass remarkably reduces the nonlinear hunting speeds while the bogie mass and specially body mass improve the hunting behavior. It was also shown that the nonlinear hunting speeds converge to the linear ones in wider tracks. It was found that any larger equivalent conicity leads to lower critical speed up to a specific conicity value ( $<0.05$ ). It was also observed that the linear model has not any remarkable sensitivity with respect to the flange clearance while the nonlinear hunting speed is significantly influenced by it. It was also proved that yaw springs can still preserve their effectiveness in hunting control even in presence of nonlinear elements and flange clearance.

## REFERENCES

- [1] Knothe K and Bohm F. History of stability of railway and road vehicles. *J Vehicle System Dynamics* 1999; 31: 283-323.
- [2] Knudsen C, Slivsgaard E, Rose M, True H and Feldberg R. Dynamics of a model of a railway wheelset. *J Nonlinear Dynamics* 1994; 6: 215-236.
- [3] Ahmadian M and Yang S. Effect of system nonlinearities on locomotive bogie hunting stability. *J Vehicle System Dynamics* 1998; 29: 365-384.
- [4] Ahmadian M and Yang S. Hopf bifurcation and hunting behavior in a rail wheelset with flange contact. *J Nonlinear Dynamics* 1998; 15: 15-30.
- [5] Yabuno H, Okamoto T and Aoshima N. Stabilization control for the hunting motion of a railway wheelset. *J Vehicle System Dynamics* 2001; 35: 41-55.
- [6] Yabuno H, Takano H and Okamoto H. Stabilization control of hunting motion of railway vehicle wheelset using gyroscopic damper. *J Vibration and Control* 2008; 14: 209-230.
- [7] Scheffel H. Passive non-linear elastic suspension devices for improved hunting stability of railway bogies. *J Vehicle System Dynamics* 2003; 37: 554-564.
- [8] Molatefi H, Hecht M and Kadivar MH. Critical speed and limit cycles in the empty Y25-freight wagon. *J Rail and Rapid Transit* 2006; 220: 347-359.
- [9] Lee SY and Cheng YC. Nonlinear hunting stability analysis of high-speed railway vehicles on curved tracks. *J Heavy Vehicle Systems* 2003; 10: 344-361.
- [10] Lee SY and Cheng YC. Nonlinear analysis on hunting stability for high-speed railway vehicle tracks on curved tracks. *J Vibration and Acoustics* 2005; 127: 324-332.
- [11] Lee SY and Cheng YC. Stability analysis of high-speed railway vehicle using half-car model. *J Heavy Vehicle Systems* 2010; 17: 139-158.
- [12] Lee SY and Cheng YC. Hunting stability analysis of high-speed railway vehicle trucks on tangent tracks. *J Sound and Vibration* 2005; 282: 881-898.
- [13] Lee SY and Cheng YC. Influence of the vertical and the roll motions of frames on the hunting stability of trucks moving on curved tracks. *J Sound and Vibration* 2006; 294: 441-453.
- [14] Lee SY, Cheng YC and Chen HH. Modeling and nonlinear hunting stability analysis of high-speed railway vehicle moving on curved tracks. *J Sound and Vibration* 2009; 324: 139-160.
- [15] Sawley K, Urban C and Walker R. The effect of hollow-worn wheels on vehicle stability in straight track. *J Wear* 2005; 258: 1100-1108.
- [16] Kim P and Seok J. Bifurcation analysis on the hunting behavior of a dual-bogie railway vehicle using the method of multiple scales. *J Sound and Vibration* 2010; 329: 4017-4039.
- [17] Zhai W, Wang K and Cai C. Fundamentals of vehicle-track coupled dynamics. *J Vehicle System Dynamics* 2009; 47: 1349-1376.
- [18] Zhai W and Wang K. Lateral hunting stability of railway vehicles running on elastic track structures. *J Computational and Nonlinear Dynamics* 2010; 5: 1-9.
- [19] Shabana AA and Sanborn G. An alternative simple multibody system approach for modelling rail flexibility in railroad vehicle dynamics. *Proc. IMechE, Part K: J. Multi-body Dynamics* 2009; 223: 107-120.
- [20] Sanborn G, Tobaa M and Shabana AA. Coupling between structural deformations and wheel-rail contact geometry in railroad vehicle dynamics. *Proc. IMechE, Part K: J. Multi-body Dynamics* 2008; 222: 381-392.

- [21] Ashtiani IH, Abedi M, Younesian D and Esmailzadeh E. Effect of partially-filled containers in dynamic behavior of tanker trains traveling on curved tracks. Proceedings of the ASME International Design Engineering Technical Conferences and Computers and Information in Engineering Conference, DETC 2008; 5: 739-747
- [22] Younesian D, Abedi M and Ashtiani IH. Dynamic analysis of a partially filled tanker train travelling on a curved track. Int. J. Heavy Vehicle Systems 2010; 17: 331-358.
- [23] Dukkupati RV. Vehicle Dynamics. 1st ed. India: Narosa, 2000.
- [24] Nayfeh AH and Mook DT. Nonlinear Oscillations. 1st ed. Berlin: Wiley-Interscience, 1995, p.720.
- [25] Durali M and Jalili MM. A new criterion for assessment of train derailment risk. Proc. IMechE, Part K: J. Multi-body Dynamics 2010; 224: 83-101.
- $W_A$  : Axle load
- $X$  : Wagon lateral displacement
- $Y$  : Wheelset lateral displacement
- $Z$  : Bogie lateral displacement
- $\Psi$  : Wheelset yaw displacement
- $\Omega$  : Hunting frequency
- $\delta$  : Clearance between wheel flange and rail
- $\varepsilon$  : Small factor
- $\theta$  : Phase shift
- $\lambda$  : Wheelset conicity
- $\mu$  : Perturbation of speed
- $\omega$  : Fundamental natural frequency for linearized system

### Nomenclature

- $a$  : Half of the track gauge
- $b$  : Half of the yaw spring arm
- $C_1, C_2, C_3$ , and  $C_4$ : Damping coefficients for primary yaw dampers
- $C_y$  : Lateral damping of primary suspension
- $C_{y2}$  : Lateral damping of secondary suspension
- $d$  : Half of the track gauge
- $f_{11}$  : Lateral creep force coefficient
- $f_{12}$  : Lateral spin creep force coefficient
- $f_{22}$  : Spin creep force coefficient
- $f_{33}$  : Longitudinal creep force coefficient
- $I_{wx}$  : Roll moment of inertia of wheelset
- $I_{wy}$  : Spin moment of inertia of wheelset
- $K_r$  : Lateral rail stiffness
- $K_w$  : Stiffness of dead-band flange force
- $K_y$  : Lateral stiffness of primary suspension
- $K_{y2}$  : Lateral stiffness of secondary suspension
- $K_\Psi$  : Yaw spring stiffness of primary suspension
- $m_B$  : Bogie mass
- $m_C$  : Wagon mass
- $m_w$  : Wheelset mass
- $r_0$  : Wheel radius
- $V_C$  : Linear critical speed
- $V_\Psi$  : Relative velocity of the longitudinal yaw damper